Neurobiology of Disease **8,** 822–833 (2001)
doi:10.1006/nbdi.2001.0423, *available online at http://www.idealibrary.com on* IDEAL®

A Murine Dopamine Neuron-Specific cDNA Library and Microarray: Increased COXI Expression during Methamphetamine Neurotoxicity[1]

Tanya Barrett,* Tao Xie,† Yulan Piao,‡ Ora Dillon-Carter,§ George J. Kargul,‡ Meng K. Lim,‡ Francis J. Chrest,* Robert Wersto,* Daniel L. Rowley,* Magdalena Juhaszova,* Li Zhou,* Marquis P. Vawter,§ Kevin G. Becker,* Christopher Cheadle,* William H. Wood III,* Una D. McCann,¶ William J. Freed,§ Minoru S. Ko,‡ George A. Ricaurte,† and David M. Donovan*

**Research Resources Branch, and ‡Laboratory of Genetics, Intramural Research Program, National Institute on Aging, 5600 Nathan Shock Drive; and §Cellular Neurobiology Branch, National Institute on Drug Abuse, National Institutes of Health, 5500 Nathan Shock Drive, Baltimore, Maryland 21224-6825; and †Department of Neurology and ¶Department of Psychiatry and Behavioral Sciences, Johns Hopkins School of Medicine, Baltimore, Maryland 21205*

Received February 20, 2001; revised April 24, 2001; accepted for publication June 4, 2001

Due to brain tissue heterogeneity, the molecular genetic profile of any neurotransmitter-specific neuronal subtype is unknown. The purpose of this study was to purify a population of dopamine neurons, construct a cDNA library, and generate an initial gene expression profile and a microarray representative of dopamine neuron transcripts. Ventral mesencephalic dopamine neurons were purified by fluorescent-activated cell sorting from embryonic day 13.5 transgenic mice harboring a 4.5-kb rat tyrosine hydroxylase promoter–*lacZ* fusion. Nine-hundred sixty dopamine neuron cDNA clones were sequenced and arrayed for use in studies of gene expression changes during methamphetamine neurotoxicity. A neurotoxic dose of methamphetamine produced a greater than twofold up-regulation of the mitochondrial cytochrome *c* oxidase polypeptide I transcript from adult mouse substantia nigra at 12 h posttreatment. This is the first work to describe a gene expression profile for a neuronal subtype and to identify gene expression changes during methamphetamine neurotoxicity.

Key Words: **dopamine; cDNA library; cDNA microarray; methamphetamine; development; gene expression profile.**

INTRODUCTION

Brain dopamine (DA)[2] neurons play a key role in movement (Bhatia & Marsden, 1994) and cognition (Robbins, 1997) and are known to mediate the reinforcing effects of drugs of abuse (Koob, 2000). In addition to their importance in normal brain function, DA neurons have been implicated in several neuropsychiatric illnesses including Parkinson's disease (Bernheimer *et al.*, 1973), schizophrenia (Carlsson *et al.*,

[1] Dopamine neuron gene sequences have been deposited in the GenBank database (Accession Nos. BE824469–BE825132).

[2] Abbreviations used: β-gal, β-galactosidase; cDNA, complementary DNA; FACS, fluorescence-activated cell sort; E13.5, embryonic day 13.5; EST, expressed sequence tag; FDG, fluorescein di-β-d-galactoside; TH, tyrosine hydroxylase; THB, tyrosine hydroxylase promoter–*lacZ* fusion transgenic mouse; METH, methamphetamine; VM, ventral midbrain; COX1, cytochrome *c* oxidase polypeptide I.

0969-9961/01 $35.00

2000), and drug addiction (Koob, 2000). Further, there is a well-described loss of DA neurons with age (Bäckman *et al.,* 2000).

Despite the wealth of data implicating brain DA neurons in normal and abnormal brain function, the molecular genetic characteristics of DA neurons remain largely unknown. In large part, the dearth of information about molecular genetic features of DA neurons is related to the difficulty of isolating pure DA neurons due to the cellular heterogeneity of brain tissue (Geschwind, 2000) and the challenge of identifying and evaluating large numbers of DA neuron-selective gene products in a time- and cost-efficient manner. However, with the advent of microarray technologies (Lee *et al.,* 2000; Sandberg *et al.,* 2000; Wada *et al.,* 2000; Yoshikawa *et al.,* 2000) and near completion of the human genome project, molecular approaches to studying human disease are undergoing a paradigm shift. Soon, it will be possible to catalogue gene expression changes for virtually every gene from normal and diseased tissues.

Methamphetamine (METH) is a potent psychomotor stimulant drug that has high potential for abuse and is known to damage brain DA neurons in animals (Seiden & Ricaurte, 1987; Villemagne *et al.,* 1998) and, possibly, humans (McCann *et al.,* 1998). Although the mechanism of METH neurotoxicity has not been identified, extensive studies implicate endogenous DA (Gibb & Kogan, 1979; Wagner *et al.,* 1983; Schmidt *et al.,* 1985; O'Dell *et al.,* 1991; Gibb *et al.,* 1994; Wrona *et al.,* 1997; Lew *et al.,* 1998), with temperature perhaps playing an important role (Bowyer *et al.,* 1992, 1994; Ali *et al.,* 1994; Albers & Sonsalla, 1995; Callahan & Ricaurte, 1998; Clausing & Bowyer, 1999; Xie *et al.,* 2000). A role of endogenous DA in METH neurotoxicity is further suggested by the finding of increased formation of DA-derived reactive oxygen species in the setting of METH intoxication (Cubells *et al.,* 1994; Cappon *et al.,* 1996; Huang *et al.,* 1997; Fumagalli *et al.,* 1998; Yamamoto & Zhu, 1998) and the increased sensitivity of VMAT2 knock-out mice to METH-induced DA neurotoxicity (Fumagalli *et al.,* 1999). Accumulating evidence also indicates that energy depletion may play a role in METH neurotoxicity (Huang *et al.,* 1997; Stephans *et al.,* 1998; Burrows *et al.,* 2000).

This work describes the use of transgenic technology to purify embryonic ventral mesencephalic dopaminergic neurons, using a fluorescent-activated cell sorting (FACS) approach similar to Abe *et al.* (1998). These purified neurons were used to create a cDNA library from which an initial dopamine neuron gene expression profile and cDNA microarray were generated. The dopamine neuron array was utilized to examine neurotoxic METH-induced changes in ventral midbrain gene expression. We now report (1) successful purification of brain DA neurons, (2) creation of a DA-cell-specific cDNA library, (3) an initial neurotransmitter-specific (DA) neuronal gene expression profile, (4) construction of a DA neuron microarray, and (5) use of the microarray to implicate regulated mitochondrial gene expression (twofold up-regulation of cytochrome oxidase I, COX1) in the molecular mechanisms underlying the neurotoxicity of methamphetamine, a drug believed to exert its effects through brain DA.

METHODS

Transgenic mouse production. The 4.5-kb rat TH promoter–*lacZ* fusion (THB) was constructed from p4.8THO (Dr. Chikaraishi, Duke University, Durham, NC) and pNASSβ (Clontech Laboratories Inc., Palo Alto, CA) using standard techniques. The TH–*lacZ* harboring DNA fragment was injected into B6D2F1 $\times$ B6C3F1 embryos. Genotyping for the transgene was by standard PCR amplification of *lacZ* sequences from tail DNA. Animals were housed and maintained in accordance with the National Institutes of Health guidelines for the care and use of laboratory animals. For embryonic studies, vaginal plug detection was assigned day 0.5.

Primary embryonic mesencephalic cells. Isolation of embryonic mesencephalic tissue was carried out as described previously (Takeshima *et al.,* 1996) with no fetal bovine serum added.

FACS. E13.5 mesencephalic tissues were triturated to single-cell suspensions in 300 μl DMEM/F12 (Life Technologies, Rockville, MD). Substrate was loaded by hypotonic shock for 45 s at 37°C by addition of 200 μl 2 mM fluorescein di-β-d-galactoside (FDG; Molecular Probes, Inc., Eugene, OR) in water and stopped with 5 ml ice-cold DMEM/F12 containing 5 mM propidium iodide (Sigma–Aldrich Corp., St. Louis, MO). Flow cytometric analysis and cell sorting was performed at 4°C using a FACStar^{Plus} cell sorter equipped with an argon laser tuned at 488 nm excitation (Becton Dickinson Immunocytometry Systems, San Jose, CA). β-Gal-expressing cells were detected with a 530DF30 filter. Dead cells were excluded by propidium iodide staining and detection with a 575DF26 filter. Data collection, analysis, and cell sorting were performed using CellQuest software (Becton Dickinson Immunocytometry Systems).

In situ β-gal and TH detection in primary cell cultures and tissues. THB$^+$ mesencephalic tissue blocks and cultured cells were labeled with fluorescent substrates as described above. Immunohistochemical analysis was performed using indirect immunofluorescence (Schachner, 1983; Poltorak *et al.*, 1992). Neurons were imaged with a Zeiss LSM-410 inverted confocal microscope (Carl Zeiss, Inc., Germany). Krypton–argon laser activation and recording wavelengths were 488 and >515 nm and 568 and >590 nm for FDG and rhodamine red, respectively. A Zeiss 63× NA 1.4 oil immersion objective was used. *In situ lacZ* detection on embryonic brains with X-gal was as described (Foran & Peterson, 1992), without fixation.

cDNA library construction and DNA sequence analysis. Approximately 3000 β-gal$^+$ cells were FACS sorted directly into 200 ml DMEM/F12 medium and stored at −80°C. RNA was isolated and the cDNA library was constructed essentially as described previously (Ko *et al.*, 2000). 3′ end sequencing of 960 clones utilized an ABI 377 Sequencer (U. Washington, St. Louis, MO). Only sequences >49 bp containing a poly(T) tract and a linker site were submitted to GenBank dbEST. The vector, linker site, and poly(T) tract sequences were removed; repetitive elements were masked; and sequences were compared by BLAST (version 2.012) (Altschul *et al.*, 1997) against the nonredundant (nr), dbEST, and Swissprot databases.

cDNA microarray construction. Bacterial plasmid DNA was isolated using 96-well alkaline lysis miniprep kits (Edge Biosystems, Gaithersburg, MD). The National Institute on Aging neuroarray clones (purchased from Research Genetics, Huntsville, AL) are listed at http://www.grc.NIA.NIH.gov/BRANCHES/RRB/DNA/DNAPUBS.htm. PCR amplification, preparation of cDNA inserts, and array construction were carried out essentially as described previously (Tanaka *et al.*, 2000), except that duplicate gene sets were printed on each array.

RNA isolation, probe production, array hybridizations, and data analyses. Total RNA was isolated from frozen tissue with TRIzol (Life Technologies). Radiolabeled probes were synthesized from 10 μg total RNA using the method described previously (Tanaka *et al.*, 2000). PCR-amplified DA cDNA was radiolabeled using Radprime DNA labeling kit (Life Technologies). Array membranes were prehybridized for 4 h at 50°C in 4 ml Microhyb hybridization buffer (Research Genetics), 100 μg human Cot-1 DNA (Life Technologies), and 40 μg polyadenylic acid (Sigma) in 50-ml Falcon tubes. Heat-denatured probe was hybridized overnight at 50°C in a rotating hybridization oven. Membranes were washed at 50°C, 2 × 15 min, with 2× SSC/0.1% SDS and exposed to bleached phosphor screens for between 1 and 5 days. Image acquisition and quantification were carried out using a phosphorimager Storm 860 system and ImageQuant software (Amersham Pharmacia, Piscataway, NJ). Replicates were performed using the same starting RNA labeled separately at least two times, except that findings on differential expression of genes associated with METH were replicated using entirely new RNA samples from comparably treated animals. In addition, each membrane contained duplicate copies of the gene set. Therefore, all array data reflect the average intensities of at least four replicated gene set hybridization results. Coefficient of variation values were calculated to determine the reliability between duplicate gene sets both within an array and between replicate experiments. Overall differences in gene expression between samples were calculated by a global normalization method based on total intensity counts for each membrane. A normalization factor was determined by dividing the average total intensity by the true total intensity. Each spot was multiplied by its appropriate normalization factor and differences were calculated as ratios from the normalized values. Background levels were determined to be uniform across each membrane and were not subtracted from the calculations. Statistical analyses and data presentation were performed using MS Excel and SpotFire Pro 4 (Spotfire, Inc., Cambridge, MA) software.

METH neurotoxicity studies. Ten mice were used for each treatment (METH and saline control). A 45 mg/kg neurotoxic dose of METH was given sc, a dose known to produce at least 60–70% reduction in nigrostriatal DA axons at 1 week (Fukumura *et al.*, 1998; Fumagalli *et al.*, 1998; Xie *et al.*, 2000). Brain regions were dissected and rapidly frozen, 12 h after METH treatment. Substantia nigra tissue samples were pooled, total RNA was extracted and radiolabeled, and microarray hybridization expression patterns were analyzed as above. Two additional groups of six mice each were treated identically, but sacrificed 1 week later, and loss of nigrostriatal DA axonal markers (striatal DA and its metabolite dihydroxyphenylacetic acid, DOPAC) was measured using HPLC (Ricaurte *et al.*, 1992).

RESULTS

The THB transgenic mouse was produced with a 4.5-kb rat TH promoter fused to lacZ (Fig. 1a). This

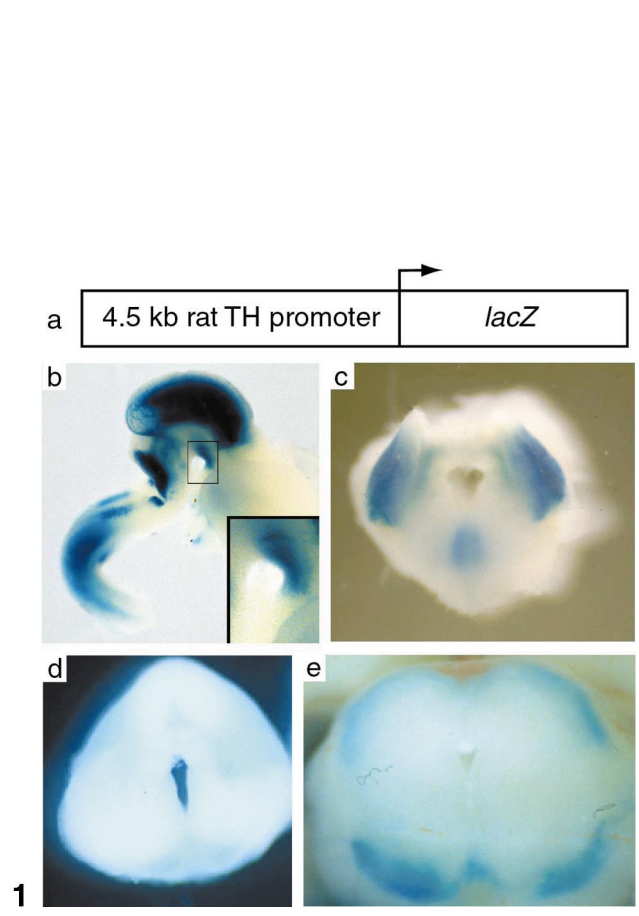

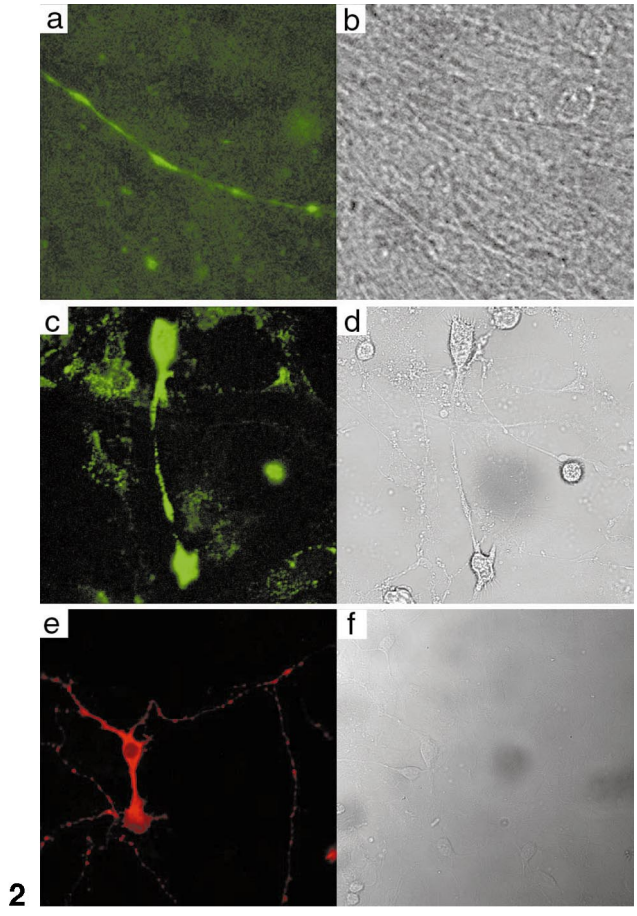

FIG. 1. THB transgene construct and *in situ* expression of β-gal. (a) 4.5-kb rat TH promoter fused to *lacZ* reporter. (b) β-Gal staining in THB E13.5 whole brain reveals expression in mesencephalic flexure (inset), as well as ectopic expression in tectum and cerebellum. (c–e) Coronal section of THB ventral midbrain at E13.5, E15.5, and E18.5, respectively. The pattern of *lacZ* expression develops over time in a manner anatomically and temporally consistent with known dopaminergic localization.

FIG. 2. Fluorescent staining of THB E13.5 VM. Primary cultures and tissue squash preparations reveal β-gal-positive cells with fluorescent cell bodies, dendrites, and varicosities typical of dopaminergic morphology. Fluorescent and bright field (a, b) FDG-stained THB E13.5 VM tissue squash preparation. Fluorescent and bright field (c, d) FDG-stained THB E13.5 VM primary culture. Fluorescent and bright field (e, f) TH immunohistochemistry of duplicate THB E13.5 VM primary culture.

promoter fragment has been used extensively by several groups to express heterologous cDNAs to dopaminergic loci of transgenic mice ventral midbrain (Banerjee *et al.*, 1992; Donovan *et al.*, 1999). β-Gal was expressed in the VM flexure of E13.5 embryos (Figs. 1b and 1c) from several founder lines (data not shown) that persisted through at least day E18.5, demonstrating DA cell localization (Figs. 1b–1e). An identical embryonic expression pattern was noted for a TH4.5-alkaline phosphatase mouse (Schimmel *et al.*, 1999).

Tissue squash preparations (Figs. 2a and 2b) and primary cultures (Figs. 2c and 2d) were prepared from the E13.5 ventral mesencephalic region of THB transgenic mice and stained with the fluorescent β-gal substrate FDG. In both cases, FDG staining revealed fluorescent green cell bodies and dendrites with varicosities typical of DA neuron morphology. Similar preparations from nontransgenic mice did not stain (data not shown). The β-gal-positive neurons occurred at a low frequency, consistent with the low number of DA neurons in the VM (predicted to be 5–10% in adult tissue). Similar numbers of TH-positive cells were obtained with identical VM cultures (Figs. 2e and 2f).

For production of embryos for FACS analysis, CD1 female mice were mated to either THB^- (negative control) or THB^+ littermate males. Figure 3 depicts representative FACS analysis of E13.5 VM tissues with high fluorescing cells from litters harboring THB^+ em-

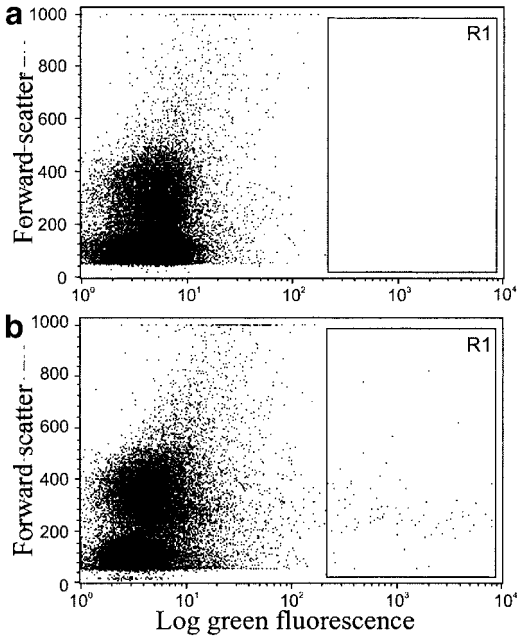

FIG. 3. FACS analysis of E13.5 THB VM FDG-stained cells. (a) THB-negative control and (b) THB-positive sample yields approximately 0.2% β-gal-positive cells. The R1 box represents the collected cell fraction.

bryos, but none from THB^- litters. Forward scatter values of the fluorescein-positive cells are consistent with the size of neuronal cells (Aller *et al.*, 1997). Fetal bovine serum was omitted from the isolation procedure in order to avoid bias in transcriptional activity and mRNA content (Iyer *et al.*, 1999). Although TH immunohistochemistry revealed 8% positive cells in pre-FACS cultures (data not shown), omission of serum is known to result in poor survival of DA cells (Takeshima *et al.*, 1996) and may explain why highly green fluorescent cells represented only 0.05–0.25% of the FACS-analyzed population. Alternatively, the DA neurons may be highly sensitive to the FACS procedure. It was a goal of this work to confirm the dopaminergic nature and origin of the effluent cells via immunohistochemical double labeling for lacZ and E13.5 dopaminergic cell markers such as TH. However, these experiments were not performed because the post-FACS cells could not be maintained in culture, despite several different culturing attempts including the use of dopamine depleted ventral midbrain feeder cell layers and preconditioned media. Approximately 500–2500 fluorescent DA neurons were collected from an average litter of 12 embryos.

From approximately 3000 FACS-purified DA neurons, RNA was extracted and a DA neuron cDNA library was created using a modified method designed for low sample amounts (Ko *et al.*, 2000). The average insert size was approximately 2 kb. 3′ DNA sequence analysis of 960 randomly selected clones identified 664 clones which contained both a poly(A) tract and linker site and were >49 bp in length. These 664 clones were clustered based on their top accession number hit according to a BLAST search against the nr database, into 288 unique, nonredundant groups, and collectively constitute an initial DA neuron gene expression profile. Of the 288 unique clusters, 85 (30%) were novel expressed sequence tags (ESTs; BLAST score >200 against nr and dbEST databases), 105 (36%) were previously identified ESTs, and 95 (34%) were named cDNAs (see Table 1 for complete list). Many neuronal-selective genes, such as neurofilament, drebrin, secretogranin II, and tau, were identified. Notably, no genes characteristic of glial cells, astrocytes, fibroblasts, endothelial cells, or nondopaminergic neurons were identified. The 960 DA cDNAs were PCR amplified and arrayed in duplicate at high density on nylon membranes to create the DA-neuron-specific cDNA microarray, in the knowledge that there were many redundancies. Due to the low yield of purified DA cells, RNA-generated probe was not available from this pool. However, in order to assign a qualitative expression level to the DA cDNA clones, prelibrary DA neuron cDNAs were PCR amplified and ^{33}P-labeled to generate probe. This hybridization pattern on the DA neuron array was compared to the pattern derived from radiolabeled E13.5 whole VM RNA in order to generate a profile of genes expressed in DA cells relative to the surrounding heterogeneous VM tissue. Due to the heterogeneous source of probe (PCR-amplified cDNA vs RNA) this comparison should only be interpreted qualitatively, with the highest DA neuron signals derived from clones of secretogranin II and the CTD-binding SR-like protein rA8 (see http://www.grc.NIA.NIH.gov/BRANCHES/RRB/DNA/DNAPUBS.htm for complete results).

Although DNA sequence analysis of the DA neuron clones verifies the high quality of the cDNA library and its neuronal origin, it is a very inefficient method to generate a comprehensive DA neuron gene expression profile. In order to expand the DA neuron gene expression profile, a second microarray was constructed with 1100 human cDNAs (National Institute on Aging neuroarray). Probes were constructed as described above from E13.5 VM total RNA, and predopamine library cDNAs and hybridized to the human NIA neuroarray. Comparison of these hybridiza-

TABLE 1

Summary of Named Genes (BLAST >200) from Dopamine Cell cDNA Library DNA Sequence Analysis

Putative ID	Accession no.	Copy no.
Neurotrophic		
Preproneurve growth factor homolog	S83440.1	1
Neurotrophic tyrosine kinase, receptor, type 2	NM_008745.1	2
Neuronal		
Brain neurofilament-L	M20480.1	2
Tau microtubule-associated protein	X79321.1	1
Drebrin A	X59267.1	1
Secretogranin II	X68837.1	6
P311	X70398.1	3
Resiniferatoxin-binding protein	X67877.1	1
Brain		
KIAA1194 protein	AB033020.1	7
KIAA0332	AB002330.1	7
KIAA0660 protein	AB014560.1	1
I54	X61497.1	1
E46 protein	X61506.1	1
Stress		
HSPC116	AF161465.1	1
HSPC061	AF161546.1	2
Heat shock protein, 84 kDa 1	NM_008302.1	5
Mitochondrially encoded		
Cytochrome *c* oxidase polypeptide I	NC_001569.1	37
Cytochrome *c* oxidase polypeptide III	NC_001569.1	3
NADH ubiquinone oxidoreductase chain 2	NC_001569.1	2
NADH ubiquinone oxidoreductase chain 4	NC_001569.1	29
NADH ubiquinone oxidoreductase chain 5	NC_001569.1	1
NADH ubiquinone oxidoreductase chain 6	NC_001569.1	22
ATP synthase A chain (protein 6)	NC_001569.1	2
Cytochrome B	NC_001569.1	4
Nuclear/transcriptional		
Nurr2	AB014889.1	3
Nuclear-binding factor NF2d9	U20086.1	1
CTD-binding SR-like protein rA8	U49055.1	26
Upstream-binding protein 1	NM_013699.1	1
Capping protein α 2	NM_007604.1	2
Matrin 3	M63485.1	1
4.5 LIM domains 1	NM_010211.1	4
Fus-associated protein with serine-arginine repeats	NM_010178.1	1
Homeobox prox 1	AF100755.1	1
Forkhead box A1	NM_008259.1	8
Zinc RING finger protein SAG	AF092877.1	1
N-myc downstream regulated 3	NM_013865.1	1
Nucleolin	X07699.1	1
PTB-like protein	AJ010585.1	8
SWI/SNF related, matrix associated, actin dependent	NM_011418.1	2
Small zinc finger-like protein	AF150101.1	2
Splicing factor, arginine/serine-rich 7	NM_006276.2	1
Nuclear ribonucleoprotein H	Y14196.1	1
Nuclear protein 220	NM_008717.1	1
Sid393p	AB025049.1	1
Structural/transport		
Tubulin, α1	NM_011653.1	5
Tubulin, β5	NM_011655.1	6
Kinectin 1	NM_008477.1	12
γ-actin	L21996.1	4
Lipid/membraneous		
Thrombin receptor	U36757.1	1
Putative membrane-associated progesterone receptor	AF042491.1	2
Katanin p60	NM_011835.1	
Membrane protein TMS-2	AF181685.1	1
Prominin	NM_008935.1	1
Keratinocyte lipid-binding protein	NM_010634.1	1
Serine palmitoyltransferase	U27455.1	4
Intracell signaling		
RalBP1-associated Eps domain-containing protein	NM_009048.1	8
Serum/glucocorticoid-regulated kinase	NM_011361.1	1
Calcium/calmodulin-dependent protein kinase-related	AF045469.1	2
F1F0-ATP synthase	Y17223.1	1
Protein phosphatase 2A	AF180350.1	1
Myristoylated alanine-rich protein kinase C substrate	NM_008538.1	1
G-protein XLAS	AF116268.1	5
Protein F1 substrate of protein kinase C	X06338.1	2
Calcineurin A1	M29550.1	2
ATP synthase, nuclear	AF030559.1	1
Ubiquitin-like		
Ubiquitin protein ligase Nedd-4	U96635.1	2
Ubiquitin-like 1	NM_009460.1	1
Ubiquitin-conjugating enzyme, 14 kDa	U04308.1	1
Ubiquitin-conjugating enzyme, mUBC9	U76416.1	5
Mitochondrial—nuclear encoded		
Sid2057p	AB025407.1	1
Malate dehydrogenase, mitochondrial	NM_008617.1	2
Mitochondrial proton/phosphate symporter	M23984.1	1
Immunological		
CDK101	Y17320.1	1
FKBP-associated protein	NM_007070.1	2
Translational/ribosomal		
Ribosomal protein L6	NM_011290.1	2
Btk locus, α-d-galactosidase A	U58105.1	2
Elf-4AII	X12507.1	1
Translation repressor Nat1	U76112.1	3
Ribosomal protein L29	NM_009082.1	1
EF 1-α	X13661.1	8
Glycyl-tRNA synthetase	NM_002047.1	4
Acidic ribosomal phosphoprotein PO	NM_007475.1	1
Housekeeping		
Tyrosine 3-monooxygenase/tryptophan 5-monooxygenase	NM_009536.1	3
Succinate dehydrogenase	AF095936.1	1
P97 ATPase pseudogene	AF122048.1	1
Triosephosphate isomerase	NM_009415.1	1
Chaperonin subunit 2	NM_007636.1	8
Glutamate dehydrogenase	NM_008133.1	1
Chaperonin subunit 4	NM_009837.1	5
Metallothionein-1 pseudogene A	M11796.1	1
Phosphoglycerate mutase type B	S63233.1	1
S-Adenosylmethionine decarboxylase	AB025024.1	1
Farnesyl diphosphate farnesyl transferase 1	NM_010191.1	1
Other		
Dixin-1	AB029448.1	6
DDP1 deafness dystonia protein 1	AB031055.1	1
Arsenite-resistance protein	U41500.1	1
Sua1	AB024303.1	3
AF1q	U95498.1	2
KIAA0196	D83780.1	4

Note. Copy number denotes the number of homologous but nonidentical (referred to as redundant) clones found among the 960 randomly selected colonies.

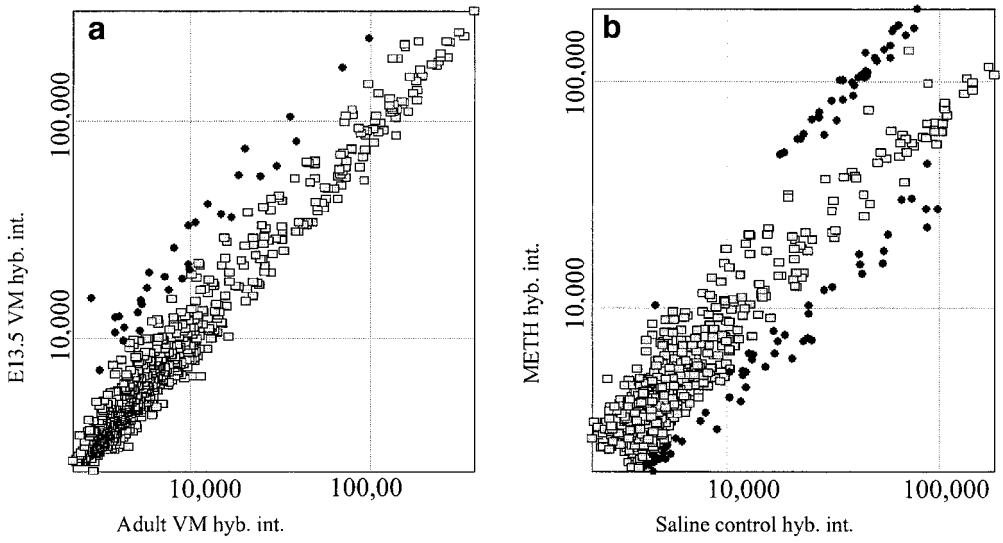

FIG. 4. Scatter plot representations of DA microarray hybridization data. (a) E13.5 VM RNA probe vs adult VM RNA probe. Fold changes were calculated for each cDNA using average values from three independent RNA labelings and membrane hybridizations (six gene set replicates in total) for each sample. (b) METH-regulated gene expression. Fold changes were calculated for each cDNA using average values from two independent RNA labelings and membrane hybridizations (four gene set replicates in total) for each sample. Dark circles represent clones whose expression increased or decreased at least twofold.

tion patterns expands the qualitative profile of genes that are expressed in the DA fraction compared to the cellularly heterogenous VM tissue and is presented as an extension of the DA neuron gene expression profile described above (see http://www.grc.NIA.NIH.gov/BRANCHES/RRB/DNA/DNAPUBS.htm. for results). This NIA-neuroarray-generated profile agreed well with the sequence-generated profile. Clones with high hybridization signals from DA cell generated probe (on NIA neuroarray) were also present in high numbers of independent clones among the sequenced isolates (e.g., α-tubulins and RalBP1-associated Eps-domain-including protein). Other clones with higher hybridization signals (on the NIA neuroarray) from DA cell cDNA-generated probe included additional Rho- and Ras-related small GTP-binding proteins and nerve growth factor receptor.

In order to evaluate the fetal derived DA array for its usefulness in studying adult tissue, we compared hybridization patterns on the DA neuron array between radiolabeled adult (3–6 months of age) vs embryonic (E13.5) VM RNA (Fig. 4a, Table 2). Only 12 of 420 unique genes showed a higher embryonic expression. No clones demonstrated higher expression in adult tissue. Similar hybridization intensities between multiple redundant clones gave added confidence to these results. The 12 genes demonstrating embryonic-enhanced expression included structural and translational machinery transcripts as expected of growing neurons with rapidly extending processes (Miller *et al.,* 1987). The lack of large numbers of embryonic enhanced clones indicates that the DA array is also representative of adult DA neuron expression and

TABLE 2

Summary of 12 Genes with Significant (Greater Than Twofold) Differential Expression in E13.5 VM vs Adult VM Found Using Dopamine Neuron Array

Putative ID (or clone accession No.)	No. copies on array	Δ E13.5 average fold (SD)
Tubulin, α1	5	↑ 2.8 (±0.6)
Tubulin, β5	6	↑ 2.6 (±0.7)
γ-Actin	4	↑ 2.5 (±0.6)
EF-1-α	8	↑ 2.3 (±0.8)
Myristoylated alanine-rich protein kinase C substrate	1	↑ 3.0
Acidic ribosomal phosphoprotein PO	1	↑ 2.2
Four previously identified ESTs (BE824606, BE824492, BE824732, BE825056)	1 each	↑ 2.0–2.4
Two novel ESTs (BE824789, BE824742)	1 each	↑ 2.1–3.0

Note. Data calculated as described in the legend to Fig. 4 except that fold changes for redundant clones were summed and averaged and standard deviations were calculated.

TABLE 3

Summary of 30 METH-Regulated Genes on Dopamine Neuron Array with Greater Than Twofold Altered Expression in Substantia Nigra

Putative ID (or clone Accession No.)	No. copies on array	Δ METH average fold (SD)
Cytochrome *c* oxidase polypeptide I	37	↑ 2.4 (±0.5)
NADH dehydrogenase chain 2	2	↓ 2.1 (±0.03)
N-myc downstream regulated 3	1	↓ 2.3
Six previously identified ESTs (BE824490, BE824492, BE824525, BE824664, BE824591, BE824733)	1 each	↓ 2.0–2.4
21 novel ESTs (BE824917, BE824737, BE824488, BE824847, BE824543, BE824874, BE824514, BE824580, BE824515, BE824891, BE824908, BE824897, BE824534, BE824509, BE824540, BE824475, BE824623, BE825001, BE824801, BE824471, BE824608)	1 each	↓ 2.0–3.8

Note. Data calculated as described in the legend to Fig. 4 except that fold changes for redundant clones were summed and averaged and standard deviations were calculated.

thus can be utilized reliably in the analysis of adult paradigms.

Compared to control animals, METH-treated animals displayed a 2.4-fold increase in the mitochondrially encoded COX1 transcript in the substantia nigra. This result is strengthened by the fact that it was mimicked in 31 independent COX1 clones on the array. A >2-fold down-regulation was noted for 29 transcripts. These included another mitochondrially encoded gene NADH ubiquinone oxidoreductase, chain 2 (ND2), n-myc downstream regulated 3 (ndr3), and 26 ESTs (Fig. 4b and Table 3). The expression of the remaining 6 mitochondrially encoded transcripts on the DA neuron array did not change significantly after METH treatment. Also, the 84-kDa heat shock protein was among the top 5 up-regulated transcripts in METH-treated animals (up 1.64-fold, data not shown), in accord with the well-established METH-induced up-regulation of the 72-kDa heat shock protein (Kuperman *et al.*, 1997; Yu *et al.*, 1999). These findings have been confirmed using independent RNA samples from multiple groups of comparably treated animals that were then analyzed separately. As expected, mice treated with METH in a parallel study showed an approximate 70% loss of the DA neuron axonal markers, DA and DOPAC, after 1 week, compared to control mice treated with saline (Fig. 5).

DISCUSSION

In the present study, we purified E13.5 DA neurons from a tyrosine hydroxylase–*lacZ* fusion mouse ventral midbrain and generated a DA-neuron-specific cDNA library. The library was then used to generate an initial DA neuron gene expression profile and to construct a DA neuron-specific cDNA microarray. After establishing the utility of the DA microarray for studying adult tissues by confirming expression of its cDNAs in both adult and embryonic ventral midbrain tissue, we used the array to study gene expression after a neurotoxic dose of METH. The results implicate regulated mitochondrial gene expression (more than twofold up-regulation of COX1) in the cytotoxic action of METH.

Purification of DA neurons was used to overcome brain tissue heterogeneity which is a major impediment to the characterization of DA-neuron-specific gene expression. Several points support the contention that the FACS purification described here greatly enriches for DA neurons. First, the 4.5-kb TH promoter is known to be expressed in VM DA neurons during embryogenesis (Schimmel *et al.*, 1999). Second, the embryonic pattern of β-gal-expressing VM cell bodies, their sparse density, and characteristic morphology in both tissue squash preparations and primary cultures suggests that the green fluorescent cells in the THB^+ FACS preparations (that are absent in THB^- animals) are DA neurons. Third, characterization of the cDNA

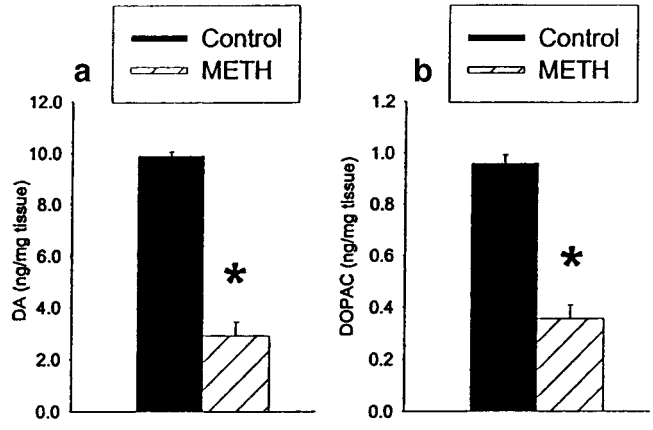

FIG. 5. Effect of METH on DA neuron axonal markers, DA (a) and DOPAC (b), in mice. Mice were treated with either METH (45 mg/kg, sc) or the same volume of saline and killed 1 week later. Values shown represent the mean ± SEM of six mice per group. *Significant difference compared to control; $P < 0.05$, determined by individual comparison after ANOVA showed an F value with $P < 0.05$.

library suggests strongly that the purified cells are neuronal in origin. Many neuronal cDNAs are identified (TrkB, prepronerve growth factor, secretogranin II, P311, drebrin A, NF-L, and tau microtubule-associated protein), while no genes indicative of a cell type other than DA neurons were identified among the sequenced clones. Also, DNA sequence analysis of 960 random cDNA clones yields an initial gene expression profile consisting of 420 nonredundant clones of which 288 have poly(A) stretches and include 95 known genes, 85 novel ESTs, and 105 previously isolated EST sequences. This high proportion of novel ESTs (30% of nonredundant clones) and neuronal cDNAs is consistent with our postulate that we isolated a rare, neuronal cell type (Ko *et al.*, 1998, 2000). Despite these supporting data, the very low yield of lacZ-labeled cells after sorting must be acknowledged. With such a low yield of cells, it is possible that the representation of genes might be skewed in some undetermined fashion or that a subset of dopamine neurons might have been purified.

Further characterization of this and other neurotransmitter-specific neuronal cell cDNA libraries will help to relieve this concern. It should also be noted that we did not find any dopaminergic-cell-specific markers among the 95 known genes identified from the 960 randomly selected clones. However, few known markers are expressed at this early time point in development (DAT and VMAT2 markers are not yet expressed in murine ventral midbrain, as extrapolated from studies in rat development; Fujita *et al.*, 1993; Hansson *et al.*, 1998) so this finding was not unexpected. This caveat not withstanding, we are confident that we have greatly enriched for dopamine neurons via the FACS purification and that this cDNA library is a much better representation of dopaminergic gene expression than was previously available.

To our knowledge, this is the first report of a neurotransmitter-specific neuronal gene expression profile. Although far from complete, this initial profile includes high levels of structural and translational machinery transcripts as expected in rapidly growing neurons as well as other genes consistent with developing DA neurons such as Trk receptors and Nurr transcription factor genes. The DNA sequence generated profile was expanded through the use of radiolabeled DA neuron-derived cDNAs hybridized to the NIA neuroarray (a microarray harboring 1100 human cDNAs). This initial profile is presented in Table 1 and at the Web sites noted under Results.

In order to evaluate the fetal derived DA array for its usefulness in studying adult tissue, comparisons were performed using VM probes generated from embryonic versus adult mice. None of the 288 nonredundant clones were uniquely expressed in the embryo, and greater than 95% of the clones demonstrate nearly identical expression levels in both adult and embryonic VM tissue, substantiating the use of this array in the study of adult conditions including aging, neuropsychiatric illness, neurodegeneration, and METH neurotoxicity.

The METH-induced neurotoxicity paradigm was chosen as a means to test the DA neuron array for its usefulness in examining neurotoxicity and DA-linked adult disorders because DA has been strongly implicated in METH neurotoxicity. Chronic doses of METH can also induce psychosis similar to schizophrenia (Sato, 1992), suggesting that METH can produce long-term changes in the brain. Although the molecular mechanism of METH neurotoxicity has not been identified, a large body of evidence suggests an essential role for endogenous DA (see Gibb *et al.*, 1994; Lew *et al.*, 1998). In addition, evidence is accumulating that energy depletion may play a role in METH neurotoxicity (Huang *et al.*, 1997; Stephans *et al.*, 1998; Burrows *et al.*, 2000). In the present studies, a neurotoxic dose of METH produced a greater than twofold up-regulation of 31 independent COX1 clones on the DA neuron array. COX1 is the mitochondrial-encoded subunit of cytochrome *c* oxidase and its up-regulation is consistent with models that implicate the generation of reactive oxygen species (possibly DA derived) (Cubells *et al.*, 1994; Cappon *et al.*, 1996; Huang *et al.*, 1997; Fumagalli *et al.*, 1998; Yamamoto and Zhu, 1998; Kita *et al.*, 1998) and/or depletion of energy in DA neurodegeneration (Huang *et al.*, 1997; Stephans *et al.*, 1998; Burrows *et al.*, 2000). COX1 catalyzes the transfer of electrons from reduced cytochrome *c* to molecular oxygen in the terminal complex (IV) of the electron transport chain (Capali, 1990). Thus, altered expression of COX1 can alter the oxidative capacity of the tissue and might represent the cells effort to increase its energy generating capacity. Although this initial study does not define the cell type where the COX1 increase occurs, increased COX1 expression exists in postmortem schizophrenic brains (Whatley *et al.*, 1996) and in the substantia nigra of Parkinson's disease (Ruberg *et al.*, 1997), suggesting that the METH-induced increase of COX1 may be DA related. The absence of METH-induced increases in other mitochondrially encoded transcripts (including COX3 from the same complex IV), and the uniquely high copy number of COX1 transcripts in the DA cDNA library, raises the intriguing possibility that this catalytic sub-

unit might serve a secondary role as an "electron scavenger."

Notably, COX1 transcript levels *increase* after METH treatment, indicating a true regulated event. Passive RNA degradation would be expected to yield decreases in transcript levels in degenerating neurons (as is seen for all other transcripts showing altered expression on the DA array). Thus, this is the first work to implicate the regulated expression of a mitochondrial electron transport protein in DA neurotoxicity. Also, the greater than twofold increase in COX1 expression occurs at the 12-h time point, when the nerve endings are committed to degradation, but before degeneration is apparent (degeneration can first be detected 18–24 h post-METH treatment). Hence, increased COX1 transcript levels might be an early indicator of DA neuron distress. It is known that COX1 can alter the oxidative capacity of the tissue and thus might also represent the cell's effort to increase its energy-generating capacity. Epidemiological studies suggest an association between agriculturally applied rotenone and Parkinson's disease incidence, adding credibility to a putative role of altered electron transport function in DA neuron degeneration (Betarbet *et al.*, 2000).

In summary, this work is the first to produce a neurotransmitter-specific neuronal cDNA library from a purified population of dopamine neurons and employ this library in the generation of both a dopamine neuron gene expression profile and a microarray representative of dopamine neuron transcripts. This technology allowed the successful characterization of gene expression changes in substantia nigra during methamphetamine neurotoxicity. Future plans are to enlarge the DA neuron microarray, to include multiple time points for METH and other animal models of neurodegenerative disorders, and to histochemically identify the cell types where the altered expression is occurring. The cataloguing of molecular responses to toxic insults will improve our understanding of the conditions and patterns of gene expression that result in DA neuron degeneration.

ACKNOWLEDGMENTS

This research was supported, in part, by grants from the National Institute on Drug Abuse (Supported by PHS Grants DA13790 and DA00206). We are indebted to Wayne French, Nancy Williams, Renee Kahn, Virginia Miller, and Donna Ritter of the Animal Resources Section, NIA, for their support in the maintenance of the mouse colony and production of timed pregnant female mice. We also thank Tom Wynn of the Photography and Arts Section, NIA, for his professional and timely help with the manuscript.

REFERENCES

Abe, K., Ko, M. S., & MacGregor, G. R. (1998) A systematic molecular genetic approach to study mammalian germline development. *Int. J. Dev. Biol.* **42,** 1051–1066.

Albers, D. S., & Sonsalla, P. K. (1995) Methamphetamine-induced hyperthermia and dopaminergic neurotoxicity in mice: Pharmacological profile of protective and nonprotective agents. *J. Pharmacol. Exp. Ther.* **275,** 1104–1114.

Ali, S. F., Newport, G. D., Holson, R. R., Slikker, W., Jr., & Bowyer, J. F. (1994) Low environmental temperatures or pharmacologic agents that produce hypothermia decrease methamphetamine neurotoxicity in mice. *Brain Res.* **658,** 33–38.

Aller, C. B., Ehmann, S., Gilman-Sachs, A., & Snyder, A. K. (1997) Flow cytometric analysis of glucose transport by rat brain cells. *Cytometry* **27,** 262–268.

Altschul, S. F., Madden, T. L., Schaffer, A. A., Zhang, J., Zhang, Z., Miller, W., & Lipman, D. J. (1997) Gapped BLAST and PSI-BLAST: A new generation of protein database search programs. *Nucleic Acids Res.* **25,** 3389–3402.

Bäckman, L., Ginovart, N., Dixon, R. A., Wahlin, T. B., Wahlin, A., Halldin, C., & Farde, L. (2000) Age-related cognitive deficits mediated by changes in the striatal dopamine system. *Am. J. Psychiatry* **157,** 635–637.

Banerjee, S. A., Hoppe, P., Brilliant, M., & Chikaraishi, D. M. (1992) 5′ flanking sequences of the rat tyrosine hydroxylase gene target accurate tissue-specific, developmental, and transsynaptic expression in transgenic mice. *J. Neurosci.* **12,** 4460–4467.

Bernheimer, H., Birkmayer, W., Hornykiewicz, O., Jellinger, K., & Seitelberger, F. (1973) Brain dopamine and the syndromes of Parkinson and Huntington: Clinical, morphological and neurochemical correlations. *J. Neurol. Sci.* **20,** 415–455.

Betarbet, R., Sherer, T. B., MacKenzie, G., Garcia-Osuna, M., Panov, A. V., & Greenamyre, J. T. (2000) Chronic systemic pesticide exposure reproduces features of Parkinson's disease. *Nature Neurosci.* **3,** 1301–1306.

Bhatia, K. P., & Marsden, C. D. (1994) The behavioural and motor consequences of focal lesions of the basal ganglia in man. *Brain* **117,** 859–876.

Bowyer, J. F., Davies, D. L., Schmued, L., Broening, H. W., Newport, G. D., Slikker, W. J., & Holson, R. R. (1994) Further studies of the role of hyperthermia in methamphetamine neurotoxicity. *J. Pharmacol. Exp. Ther.* **268,** 1571–1580.

Bowyer, J. F., Tank, A. W., Newport, G. D., Slikker, W., Jr., Ali, S. F., & Holson, R. R. (1992) The influence of environmental temperature on the transient effects of methamphetamine on dopamine levels and dopamine release in striatum. *J. Pharmacol. Exp. Ther.* **260,** 817–824.

Burrows, K. B., Nixdorf, W. L., & Yamamoto, B. K. (2000) Central administration of methamphetamine synergizes with metabolic inhibition to deplete striatal monoamines. *J. Pharmacol. Exp. Ther.* **292,** 853–860.

Callahan, B. T., & Ricaurte, G. A. (1998) Effect of 7-nitroindazole on body temperature and methamphetamine-induced dopamine toxicity. *NeuroReport* **9,** 2691–2695.

Capali, R. A. (1990) Structure and function of cytochrome c oxidase. *Annu. Rev. Biochem.* **59,** 569–596.

Cappon, G. D., Broening, H. W., Pu, C., Morford, L., & Vorhees, C. V. (1996) Alpha-phenyl-*N*-tert-butyl nitrone attenuates methamphetamine-induced depletion of striatal dopamine without altering hyperthermia. *Synapse* **24,** 173–181.

Carlsson, A., Waters, N., Waters, S., & Carlsson, M. L. (2000) Network interactions in schizophrenia—Therapeutic implications. *Brain Res. Brain Res. Rev.* **31,** 342–349.

Clausing, P., & Bowyer, J. F. (1999) Time course of brain temperature and caudate/putamen microdialysate levels of amphetamine and dopamine in rats after multiple doses of *d*-amphetamine. *Ann. N. Y. Acad. Sci.* **890,** 495–504.

Cubells, J. F., Rayport, S., Rajindron, G., & Sulzer, D. (1994) Methamphetamine neurotoxicity involves vacuolation of endocytic organelles and dopamine-dependent intracellular stress. *J. Neurosci.* **14,** 2260–2771.

Donovan, D. M., Miner, L. L., Perry, M. P., Revay, R. S., Sharpe, L. G., Przedborski, S., Kostic, V., Philpot, R. M., Kirstein, C. L., Rothman, R. B., Schindler, C. W., & Uhl, G. R. (1999) Cocaine reward and MPTP toxicity: Alteration by regional variant dopamine transporter overexpression. *Mol. Brain Res.* **73,** 37–49.

Foran, D. R., & Peterson, A. C. (1992) Myelin acquisition in the central nervous system of the mouse revealed by an MBP-lacZ transgene. *J. Neurosci.* **12,** 4890–4897.

Fukumura, M., Cappon, G., Cunfeng, P., Broening, H., & Vorhees, C. (1998) A single dose model of methamphetamine-induced neurotoxicity in rats: Effects on neostratal monoamines and glial fibrillary acidic protein. *Brain Res.* **806,** 1–7.

Fujita, M., Shimada, S., Nishimura, T., Uhl, G. R., & Tohyam, M. (1993) Ontogeny of dopamine transporter mRNA expression in the rat brain. *Brain Res. Mol. Brain Res.* **19,** 222–226.

Fumagalli, F., Gainetdinov, R. R., Valenzano, K. J., & Caron, M. G. (1998) Role of dopamine transporter in methamphetamine-induced neurotoxicity: Evidence from mice lacking the transporter. *J. Neurosci.* **18,** 4861–4869.

Fumagalli, F., Gainetdinov, R. R., Wang, Y. M., Valenzano, K. J., Miller, G. W., & Caron, M. G. (1999) Increased methamphetamine neurotoxicity in heterozygous vesicular monoamine transporter 2 knock-out mice. *J. Neurosci.* **19,** 2424–2431.

Geschwind, D. H. (2000) Mice, microarrays, and the genetic diversity of the brain. *Proc. Natl. Acad. Sci. USA* **97,** 10676–10678.

Gibb, J. W., Hanson, G. R., & Johnson, M. (1994) Neurochemical mechanisms of toxicity. In: *Amphetamine and Its Analogs* (A. K. Cho & D. S. Segal, Eds.), pp. 269–295. Academic Press, San Diego.

Gibb, J. W., & Kogan, F. J. (1979) Influence of dopamine synthesis on methamphetamine-induced changes in striatal and adrenal tyrosine hydroxylase activity. *Arch. Pharmacol.* **310,** 185–187.

Hansson, S. R., Hoffman, B. J., & Mezey, E. (1998) Ontogeny of vesicular monoamine transoreter mRNAs VMAT1 and VMAT2. I. The Developing rat central nervous system. *Brain Res. Dev. Brain Res.* **110,** 135–158.

Huang, N. K., Wan, F. J., Tseng, C. J., & Tung, C. S. (1997) Nicotinamide attenuates methamphetamine-induced striatal dopamine depletion in rats. *NeuroReport* **8,** 1883–1885.

Iyer, V. R., Eisen, M. B., Ross, D. T., Schuler, G., Moore, T., Lee, J. C. F., Trent, J. M., Staudt, L. M., Hudson, J., Jr., Boguski, M. S., Lashkari, D., Shalon, D., Botstein, D., & Brown, P. O. (1999) The transcriptional program in the response of human fibroblasts to serum. *Science* **283,** 83–87.

Kita, T., Paku, S., Takahashi, M., Kubo, K., Wagner, G. C., & Nakashima, T. (1998) Methamphetamine-induced neurotoxicity in BALB/c, DBA/2N and C57BL/6N mice. *Neuropharmacology* **37,** 1177–1184.

Ko, M. S., Kitchen, J. R., Wang, X., Threat, T. A., Wang, X., Hasegawa, A., Sun, T., Grahovac, M. J., Kargul, G. J., Lim, M. K., Cui, Y., Sano, Y., Tanaka, T., Liang, Y., Mason, S., Paonessa, P. D., Sauls, A. D., DePalma, G. E., Sharara, R., Rowe, L. B., Eppig, J., Morrell, C., & Doi, H. (2000) Large-scale cDNA analysis reveals phased gene expression patterns during preimplantation mouse development. *Development* **127,** 1737–1749.

Ko, M. S., Threat, T. A., Wang, X., Horton, J. H., Cui, Y., Wang, X., Pryor, E., Paris, J., WellsSmith, J., Kitchen, J. R., Rowe, L. B., Eppig, J., Satoh, T., Brant, L., Fujiwara, H., Yotsumoto, S., & Nakashima, H. (1998) Genome-wide mapping of unselected transcripts from extraembryonic tissue of 7.5-day mouse embryos reveals enrichment in the t-complex and under-representation on the X chromosome. *Hum. Mol. Genet.* **7,** 1967–1978.

Koob, G. F. (2000) Neurobiology of addiction: Toward the development of new therapies. *Ann. N. Y. Acad. Sci.* **909,** 170–185.

Kuperman, D. I., Freyaldenhoven, T. E., Schmued, L. C., & Ali, S. F. (1997) Methamphetamine-induced hyperthermia in mice: Examination of dopamine depletion and heat-shock protein induction. *Brain Res.* **771,** 221–227.

Lee, C. K., Weindruch, R., & Prolla, T. A. (2000) Gene-expression profile of the ageing brain in mice. *Nature Genet.* **25,** 294–297.

Lew, R., Malberg, J. E., Ricaurte, G. A., & Seiden, L. S. (1998) Evidence for and mechanism of action of neurotoxicity of amphetamine related compounds. In: *Highly Selective Neurotoxins: Basic and Clinical Applications* (R. M. Kostrzewa, Ed.), pp. 235–268. Humana Press, Totowa, NJ.

McCann, U. D., Wong, D. F., Yokoi, F., Villemagne, V., Dannals, R. F., & Ricaurte, G. A. (1998) Reduced striatal dopamine transporter density in abstinent methamphetamine and methcathinone users: Evidence from positron emission tomography studies with [^{11}C]WIN-35,428. *J. Neurosci.* **18,** 8417–8422.

Miller, F. D., Naus, C. C., Higgins, G. A., Bloom, F. E., & Milner, R. J. (1987) Developmentally regulated rat brain mRNAs: Molecular and anatomical characterization. *J. Neurosci.* **7,** 2433–2444.

O'Dell, S. J., Weihmuller, F. B., & Marshall, J. F. (1991) Multiple methamphetamine injections induce marked increases in extracellular striatal dopamine which correlate with subsequent neurotoxicity. *Brain Res.* **564,** 256–260.

Poltorak, M., Isono, M., Freed, W. J., Ronnett, G. V., & Snyder, S. H. (1992) Human cortical neuronal cell line (HCN-1): Further in vitro characterization and suitability for brain transplantation. *Cell Transplant.* **1,** 3–15.

Ricaurte, G. A., Martello, A. L., Katz, J. L., & Martello, M. B. (1992) Lasting effects of (±)-3,4-methylenedioxymethamphetamine (MDMA) on central serotonergic neurons in nonhuman primates: Neurochemical observations. *J. Pharmacol. Exp. Ther.* **261,** 616–622.

Robbins, T. W. (1997) Arousal systems and attentional processes. *Biol. Psychol.* **45,** 57–71.

Ruberg, M., Brugg, B., Prigent, A., Hirsch, E., Brice, A., & Agid, Y. (1997) Is differential regulation of mitochondrial transcripts in Parkinson's disease related to apoptosis? *J. Neurochem.* **68,** 2098–2110.

Sandberg, R., Yasuda, R., Pankratz, D. G., Carter, T. A., Del Rio, J. A., Wodicka, L., Mayford, M., Lockhart, D. J., & Barlow, C. (2000) Regional and strain-specific gene expression mapping in the adult mouse brain. *Proc. Natl. Acad. Sci. USA* **97,** 11038–11043.

Sato, M. (1992) A lasting vulnerability to psychosis in patients with previous methamphetamine psychosis. *Ann. N. Y. Acad. Sci.* **654,** 160–170.

Schachner, M. (1983) Immunohistochemistry and immunocytochemistry of neural cell types in vitro and in situ. In: *Immunohistochemistry* (A. Cuello, Ed.), pp. 399–429. Wiley–Interscience, New York.

Schimmel, J. J., Crews, L., Roffler-Tarlov, S., & Chikaraishi, D. M. (1999) 4.5 kb of the rat tyrosine hydroxylase 5′ flanking sequence directs tissue specific expression during development and contains consensus sites for multiple transcription factors. *Brain Res. Mol. Brain Res.* **74,** 1–14.

Schmidt, C. J., Ritter, J. K., Sonsalla, P. K., Hanson, G. R., & Gibb, J. W. (1985) Role of dopamine in the neurotoxic effects of methamphetamine. *J. Pharmacol. Exp. Ther.* **233,** 539–544.

Seiden, L. S., & Ricaurte, G. A. (1987) Neurotoxicity of methamphetamine and related drugs. In: *Psychopharmacology—The Third Generation of Progress* (H. Y. Meltzer, Ed.), pp. 359–366. Raven Press, New York.

Stephans, S. E., Whittingham, T. S., Douglas, A. J., Lust, W. D., & Yamamoto, B. K. (1998) Substrates of energy metabolism attenuate methamphetamine-induced neurotoxicity in striatum. *J. Neurochem.* **71,** 613–621.

Takeshima, T., Shimoda, K., Johnston, J. M., & Commissiong, J. W. (1996) Standardized methods to bioassay neurotrophic factors for dopaminergic neurons. *J. Neurosci. Methods* **67,** 27–41.

Tanaka, T. S., Jaradat, S. A., Lim, M. K., Kargul, G. J., Wang, X., Grahovac, M. J., Pantano, S., Sano, Y., Piao, Y., Nagaraja, R., Doi, H., Wood, W. H., 3rd, Becker, K. G., & Ko, M. S. (2000) Genome-wide expression profiling of mid-gestation placenta and embryo using a 15,000 mouse developmental cDNA microarray. *Proc. Natl. Acad. Sci. USA* **97,** 9127–9137.

Villemagne, V., Yuan, J., Wong, D. F., Dannals, R. F., Hatzidimitriou, G., Mathews, W. B., Ravert, H. T., Musachio, J., McCann, U. D., & Ricaurte, G. A. (1998) Brain dopamine neurotoxicity in baboons treated with doses of methamphetamine comparable to those recreationally abused by humans: Evidence from [^{11}C]WIN-35,428 positron emission tomography studies and direct in vitro determinations. *J. Neurosci.* **18,** 419–427.

Wada, R., Tifft, C. J., & Proia, R. L. (2000) Microglial activation precedes acute neurodegeneration in sandhoff disease and is suppressed by bone marrow transplantation. *Proc. Natl. Acad. Sci. USA* **97,** 10954–10959.

Wagner, G. C., Lucot, J. B., Schuster, C. R., & Seiden, L. S. (1983) Alpha-methyltyrosine attenuates and reserpine increases methamphetamine-induced neuronal changes. *Brain Res.* **270,** 285–288.

Whatley, S. A., Curti, D., & Marchbanks, R. M. (1996) Mitochondrial involvement in schizophrenia and other functional psychoses. *Neurochem. Res.* **21,** 995–1004.

Wrona, M. Z., Yang, Z., Zhang, F., & Dryhurst, G. (1997) Potential new insights into the molecular mechanisms of methamphetamine-induced neurodegeneration. *NIDA Res. Monogr.* **173,** 146–174.

Xie, T., McCann, U. D., Kim, S., Yuan, J., & Ricaurte, G. A. (2000) Effect of temperature on dopamine transporter function and intracellular accumulation of methamphetamine: Implications for methamphetamine-induced dopaminergic neurotoxicity. *J. Neurosci.* **20,** 7838–7845.

Yamamoto, B. K., & Zhu, W. (1998) The effects of methamphetamine on the production of free radicals and oxidative stress. *J. Pharmacol. Exp. Ther.* **287,** 107–114.

Yoshikawa, T., Nagasugi, Y., Azuma, T., Kato, M., Sugano, S., Hashimoto, K., Masuho, Y., Muramatsu, M., & Seki, N. (2000) Isolation of novel mouse genes differentially expressed in brain using cDNA microarray. *Biochem. Biophys. Res. Commun.* **275,** 532–537.

Yu, X., Imam, S. Z., Newport, G. D., Slikker, W., Jr., & Ali, S. F. (1999) Ibogaine blocked methamphetamine-induced hyperthermia and induction of heat shock protein in mice. *Brain Res.* **823,** 213–216.